Convex-hull mass estimates of the dodo (*Raphus cucullatus)*: application of a CT-based mass estimation technique

Charlotte A Brassey, Thomas O'Mahoney, Andrew C Kitchener, Phillip L Manning, William I Sellers

The external appearance of the dodo (*Raphus cucullatus*) has been a source of considerable intrigue as contemporaneous accounts or depictions are rare. The body mass of the dodo has been particularly contentious, with the flightless pigeon alternatively reconstructed as slim or overweight depending upon the skeletal metric used as the basis for mass prediction. Resolving this dichotomy and obtaining a reliable estimate for mass is essential before future analyses regarding dodo life history, physiology or biomechanics can be conducted. Previous mass estimates of the dodo have relied upon predictive equations based upon hind limb dimensions of extant pigeons. Yet the hind limb proportions of dodo have been found to differ considerably from those of their modern relatives, particularly with regards to midshaft diameter. Therefore, application of predictive equations to unusually robust fossil skeletal elements may bias mass estimates. We present a whole-body computed tomography (CT) -based mass estimation technique for application to the dodo. We generate 3D volumetric renders of the articulated skeletons of 20 species of extant pigeons, and wrap minimum-fit 'convex hulls' around their bony extremities. Convex hull volume is subsequently regressed against mass to generate predictive models based upon whole skeletons. Our best-performing predictive model is characterized by high correlation coefficients and low mean squared error (a=-2.31, b=0.90, r^2=0.97, MSE=0.0046). When applied to articulated composite skeletons of the dodo (National Museums Scotland, NMS.Z.1993.13; Natural History Museum, NHM A.9040 and S/1988.50.1), we estimate eviscerated body masses of 8-10.8 kg. When accounting for missing soft tissues, this may equate to live masses of 10.6-14.3 kg. Mass predictions presented here fall towards the lower end of those previously published, and support recent suggestions of a relatively slim dodo. CT-based reconstructions provide a means of objectively estimating mass and body segment properties of extinct species using whole articulated skeletons.

1 **Convex-hull mass estimates of the dodo (*Raphus cucullatus*): application of a CT-**

2 **based mass estimation technique**

4   Brassey, C.A.[1]*, O'Mahoney, T.[1], Kitchener, A.C.[2], Manning, P. L.[3], Sellers, W.I.[1]

6   [1]Faculty of Life Sciences, University of Manchester, Manchester M13 9PL

7   [2]Department of Natural Sciences, National Museums Scotland, Edinburgh EH1 1JF

8   [3]Interdisciplinary Centre for Ancient Life, School of Earth, Atmospheric and

9   Environmental Sciences, University of Manchester, Manchester M13 9PL

11   *corresponding author (charlotte.brassey@manchester.ac.uk)

12 **Abstract**

13 The external appearance of the dodo (*Raphus cucullatus*) has been a source of

14 considerable intrigue as contemporaneous accounts or depictions are rare. The body

15 mass of the dodo has been particularly contentious, with the flightless pigeon

16 alternatively reconstructed as slim or overweight depending upon the skeletal metric

17 used as the basis for mass prediction. Resolving this dichotomy and obtaining a reliable

18 estimate for mass is essential before future analyses regarding dodo life history,

19 physiology or biomechanics can be conducted.

21 Previous mass estimates of the dodo have relied upon predictive equations based upon

22 hind limb dimensions of extant pigeons. Yet the hind limb proportions of dodo have

23 been found to differ considerably from those of their modern relatives, particularly with

24 regards to midshaft diameter. Therefore, application of predictive equations to unusually

25 robust fossil skeletal elements may bias mass estimates. We present a whole-body

26 computed tomography (CT) -based mass estimation technique for application to the

27 dodo. We generate 3D volumetric renders of the articulated skeletons of 20 species of

28 extant pigeons, and wrap minimum-fit 'convex hulls' around their bony extremities.

29 Convex hull volume is subsequently regressed against mass to generate predictive

30 models based upon whole skeletons.

32 Our best-performing predictive model is characterized by high correlation coefficients

33 and low mean squared error (*a*=-2.31, *b*=0.90, r^2=0.97, MSE=0.0046). When applied to

34 articulated composite skeletons of the dodo (National Museums Scotland,

35   NMS.Z.1993.13; Natural History Museum, NHM A.9040 and S/1988.50.1), we estimate

36   eviscerated body masses of 8-10.8 kg. When accounting for missing soft tissues, this

37   may equate to live masses of 10.6-14.3 kg. Mass predictions presented here fall

38   towards the lower end of those previously published, and support recent suggestions of

39   a relatively slim dodo. CT-based reconstructions provide a means of objectively

40   estimating mass and body segment properties of extinct species using whole articulated

41   skeletons.

42

43   Key words: dodo, *Raphus cucullatus,* body mass, computed tomography, convex hulls

Introduction

Body mass (M_b) is a fundamental descriptor of an organism and co-varies with important ecological and physiological traits, such as population density, metabolism and cost-of-transport [1]. Key evolutionary scenarios, such as the origin of avian flight [2] and the extinction of island flightless avian species [3], have been diagnosed on the basis of estimated M_b. Therefore, the reconstruction of body mass in extinct bird species is a subject of considerable interest within the palaeontological and evolutionary biology literature [2–6].

An often-applied technique for estimating the body mass of an extinct vertebrate has been to measure a skeletal dimension from modern species, such as femur circumference [7] or glenoid diameter [8], and apply this as the independent variable in a regression against body mass. However, 'overdevelopment' of the pelvic apparatus has been found to be significantly correlated with the flightless condition in extant birds [9]. Therefore, the application of mass prediction equations, based solely on hind limb material of flightless avian taxa, has been questioned in extinct species such as the moa [6].

The dodo (*Raphus cucullatus*) is an iconic representative of island flightlessness and human-induced extinction, and its external appearance has been a source of considerable intrigue due to the scarcity of contemporaneous accounts or depictions [10]. This extinct flightless columbiform was endemic to the island of Mauritius. However, the skeletal anatomy of the dodo is comparatively well known, and its pelvic

67   morphology has been thoroughly investigated. Hind limb bones of *R. cucullatus* have

68   been found to differ considerably in both their length and width relative to their volant

69   relatives [11, although see 12]. Yet previous attempts to estimate the body mass of the

70   dodo have predominantly relied upon predictive equations derived solely from the hind

71   limb metrics of extant species [13–15].

72   An alternative approach to mass estimation involves the reconstruction of 3D volumetric

73   models. An early volumetric reconstruction of the dodo was conducted by physically

74   sculpting a scale model of an individual and estimating volume via fluid displacement

75   [12]. Whilst such volumetric techniques are less liable to bias by individual robust/gracile

76   postcranial elements than traditional linear bivariate equations, they do inevitably

77   involve some degree of artistic licence in the sculpting of soft tissue contours and

78   require an estimate for fossil body density to be assigned.

79   Following advances in 3D imaging technology, the use of digital skeletal models in

80   mass estimation of fossil skeletons has become increasingly popular [16–19]. These

81   studies typically involve the 'wrapping' of geometric shapes or lofted smooth surfaces

82   around the skeleton in order to replicate the original soft tissue contour of the animal.

83   Zero-density cavities such as lung and tracheal space may also be modeled [20].

84   However, similar to physical sculpting with clay, assumptions must still be made

85   regarding body density and the extent of soft tissues beyond the skeleton. Therefore, it

86   is essential that reconstructions are grounded within a quantitative understanding of

87   extant species in order to avoid subjective modeling of soft tissues (both body and

88   plumage).

89 Here we present new mass estimates for the dodo based on an alternative 'convex hull'

90 volumetric reconstruction approach [21,22]. The convex hull (*CH*) of a set of points is

91 defined as the smallest convex polytope that contains all said points, and intuitively can

92 be thought of as a shrink-wrap fit around an object (see Figure 1). Application of the

93 convex hulling technique to mass estimation does not involve any subjective

94 reconstruction of soft tissue anatomy and solely relies upon the underlying skeleton. We

95 calculate minimum convex hull volumes for a sample of composite articulated dodo

96 skeletons, and convert these to body mass estimates using a computed tomography

97 (CT) calibration dataset of 20 species of extant pigeon. To our knowledge, this is the

98 first time such an extensive CT dataset of extant animals has been used to reconstruct

99 the   body   mass   of   a   fossil   of   an   extinct   species.

Methods and Materials

100

101   The modern dataset consists of 20 columbiform individuals, spanning a wide variety of

102   body sizes from a 70 g fruit dove (*Ptilinopus*) up to the largest extant pigeon, the 2 kg

103   Victoria crowned pigeon (*Goura victoria*). We also cover a broad taxonomic range

104   (including the closest extant relative of the dodo [23], the Nicobar pigeon (*Caloenas*

105   *nicobarica)*). Frozen carcasses were sourced from National Museums Scotland,

106   Edinburgh, and the University of Manchester (see Table 1). Carcasses were CT

107   scanned at Leahurst Veterinary School, University of Liverpool, in a Toshiba Aquilion

108   PRIME helical scanner at a slice thickness of 0.5mm and a pixel spacing of between

109   0.24-0.51mm, depending on the maximum size of the specimen. 3D models of the

110   skeletons were generated in Seg3D [24], using an automatic threshold with subsequent

111   manual masking to remove the dense rachises attached to the forelimb.

112

113   Models were exported into Geomagic Studio (www.geomagic.com), where each

114   skeleton was divided into functional units (skull, neck, trunk, humerus, radius+ulna,

115   carpometacarpals, femur, tibiotarsus+fibula, tarsometatarsus, feet). The cervical series

116   was further subdivided in order to achieve a tight-fitting hull around the curving neck.

117   Minimum convex hulls were calculated in MATLAB (www.mathworks.com), using the

118   'convhull' function implementing the Quickhull (qhull) algorithm [25], and total convex

119   hull volume was calculated as the sum of individual segment volumes (see Figure 1).

120   Body mass was measured for each carcass, and the relationship between M_b and

121   convex hull volume (CH_{vol}) was estimated using ordinary least squares (OLS)

122   regression on $\log_{10}$ transformed data. As the purpose of the regression was to derive a

123   predictive equation, a type-I regression, such as OLS, was deemed most appropriate

124   [26]. Additionally we accounted for the statistical non-independence of phylogenetically-

125   related data points by carrying out phylogenetic generalized least squares (PGLS)

126   regressions, implemented in MATLAB using 'Regression2' software [27]. A composite

127   phylogeny was modified from Johnson et al. [28] and Heupink et al. [29], with all branch

128   lengths equal to 1.

129

130   To reconstruct the body masses of articulated dodo skeletons, we generated 3D digital

131   models of these specimens. The Edinburgh dodo (National Museums Scotland,

132   NMS.Z.1993.13) was scanned using a Z+F Imager 5010 LiDAR (Light Detection And

133   Range) scanner and reconstructed in the Z+F LaserControl software. The Natural

134   History Museum (NHM), London specimens (Tring skeleton, S/1988.50.1; South

135   Kensington specimen NHM A9040) were digitized using the photogrammetric technique

136   detailed elsewhere [30,31] and reconstructed in VisualSFM [32]. Despite application of

137   two alternative imaging techniques, previous studies have found the results obtained via

138   photogrammetry and laser scanning to be comparable [30], and convex hull results to

139   be insensitive to point cloud density [22,33]. 3D models of the dodo skeletons were

140   cleaned up in Geomagic and subdivided into functional units. Our only intervention with

141   the dodo models was to mirror the right hand side of the Edinburgh ribcage to account

142   for missing ribs on its left side. Convex hulls were fitted according to the methodology

143   applied to modern pigeons.

Results

144

145 Total convex hull volumes for the modern pigeons are reported in Table 1, and

146 segment-specific CH_{vol} values can be found in Supplementary Material S1. Convex hull

147 models are available for download from http://www.animalsimulation.org. We found

148 considerable variation between frozen pigeon specimens in the posture of the digits

149 forming the foot i.e. adduction vs. abduction of the digits. This influenced the overall

150 shape, and hence calculated CH_{vol}, of the foot functional units (see Figure 1D). Given

151 repositioning of the skeleton was not possible due to the frozen nature of the carcasses,

152 here we report total CH_{vol} values with and without feet included. External inspection of

153 the carcasses suggested evisceration had been carried out on some specimens. Using

154 CT scans the occurrence of evisceration was confirmed across our modern dataset (see

155 Table 1). Therefore, we report separate predictive models derived from 'eviscerated'

156 carcasses (n=13), 'intact' carcasses (n=7), and a third 'combined' model comprising

157 both eviscerated and intact specimens (n=20).

158

159 The results of the OLS regression analyses are presented in Table 2, and

160 phylogenetically corrected (PGLS) regressions are given in Supplementary Material S2

161 alongside the composite phylogeny used in this analysis. PGLS regressions did not

162 provide a better fit to the data than uncorrected OLS regressions (as determined by

163 Akaike Information Criterion values, AIC) for the 'eviscerated' and 'combined' models

164 (Table 2). However, a PGLS model was found to fit the 'intact' extant pigeon data better

165 than an uncorrected OLS model (Table 2).

166

167 Removing CH_{vol} of the feet from the analyses had very little effect on the results of the

168 regression, although mean squared error (MSE) decreased slightly in all models (Table

169 2) and therefore only regression models minus feet are discussed any further in the text.

170 Figure 2 illustrates a strong positive correlation between $M_{b\ and}$ CH_{vol} for the eviscerated

171 specimens within the sample (a=-2.31, b=0.90, r^2=0.97, MSE=0.0046). In contrast, the

172 relationship between $M_{b\ and}$ CH_{vol} in intact specimens illustrates a weak positive

173 correlation characterized by low correlation coefficients and high mean square error (a=-

174 1.06, b=0.66, r^2=0.70, MSE=0.0161). Intact specimens do not plot consistently above

175 the eviscerated pigeon slope (Figure 2) and are instead characterized by a high degree

176 of scatter. When combining the eviscerated and intact specimens into one dataset, M_b

177 and CH_{vol} remain tightly correlated (a=-2.08, b=0.85, r^2=0.92, MSE=0.0084).

178

179 Total CH_{vol} calculated for the mounted dodo skeletons are reported in Table 3 (see

180 Supplementary Material S3 for segment-specific values) and an example of a

181 photogrammetric model is illustrated in Figure 3. Using the 'eviscerated' predictive

182 model, dressed M_b is estimated as 8.0 kg (95% prediction interval (PI) 4.6-13.9 kg), 8.7

183 kg (95%PI 5.0-15.0 kg) and 10.8 kg (95%PI 6.1-19.0 kg) respectively for the NHM Tring,

184 NHM South Kensington and Edinburgh dodos. Applying the 'combined' predictive

185 equation results in wider and therefore more conservative prediction intervals (NHM

186 Tring, 6.7 kg 95%PI 3.5-13.1 kg; NHM South Kensington, 7.3 kg 95%PI 3.7-14.3 kg;

187 Edinburgh, 9.0 kg 95%PI 4.5-17.9 kg).

188

189 Figure 4 illustrates the distribution of segment-specific convex hull volumes as a
190 proportion of total CH_{vol} within the models. In extant pigeons trunk CH_{vol} represents on
191 average 69% of total CH_{vol}. The NHM Tring dodo skeleton has a percentage trunk
192 volume significantly lower than that of extant pigeons (67%, 1-tailed t-test, t=3.23,
193 $p<0.01$), whilst percentage trunk volume in the NHM South Kensington and Edinburgh
194 skeletons is significantly higher than extant pigeons (71% and 80%, t=-2.23 and -13.0
195 respectively, $p<0.05$). With the exception of the tarsometatarsii of the NHM South
196 Kensington skeleton, pelvic convex hull segments of the dodos comprise a significantly
197 greater proportion of total CH_{vol} than in extant pigeons ($p<0.05$). In contrast, dodo
198 pectoral convex hull segments contribute proportionally less to total CH_{vol} than in extant
199 pigeons ($p<0.0001$) (Figure 4).

200 **Discussion**

201 ***Predictive equation derived from modern CT dataset***

202 To our knowledge the present study represents the first application of a predictive

203 equation derived solely from whole-body CT to the problem of body mass estimation for

204 extinct animals. Previous volumetric mass estimate studies have relied upon articulated

205 skeletons of extant species to derive a calibration equation [6,21]. Yet articulated

206 skeletons are often missing crucial specimen information, such as a recorded body

207 mass. By working with frozen carcasses, body mass is directly measurable and

208 uncertainties associated with mounting and posing of the skeletons can be avoided [22].

209

210 Our dataset consists of both 'intact' and 'eviscerated' pigeons as determined by

211 examination of CT scans. Previous analyses of carcass composition have found

212 eviscerated mass to represent 62-66% of live body mass in rock doves [34,35], yet no

213 data exist regarding the possible scaling of internal organ mass across a range of body

214 sizes in the Columbiformes. As can be seen in Figure 2, there is no consistent disparity

215 between intact and eviscerated specimens, and the relationship between M_b and CH_{vol}

216 in intact pigeons is relatively weak (r^2=70, p=0.019). This correlation improves

217 considerably when accounting for phylogeny (Supplementary Material S2), but remains

218 weaker than the relationship between M_b and CH_{vol} characterizing eviscerated

219 specimens. Live body mass has been shown to vary considerably in wild animals due to

220 hydration, nutrition and gut content [36] and therefore some degree of scatter is to be

221 expected in intact carcasses. Particularly striking is the variability in gizzard contents

222 between similar-sized specimens visible in CT scans (see Figure 5).

223

224   This suggests intact pigeon M_b cannot be corrected for the presence of internal organs

225   using a single factor representing average percentage eviscerated mass as a function

226   of live mass (i.e. multiplying by values of 0.62 or 0.66 previously found in the literature).

227   Additionally, attempting to correct intact M_b by substituting intact CH_{vol} into the

228   eviscerated regression model would be highly circular and result in artificially inflated

229   correlation coefficients, if the equation were used in a predictive capacity. Therefore, we

230   apply both the uncorrected OLS eviscerated model and combined (eviscerated and

231   intact) model to bracket the range of likely dodo body masses. Interestingly, the very

232   high correlation coefficient and low mean squared error of the eviscerated equation

233   (r^2=0.97, MSE=0.0046) suggest that once the variability associated with fluid and gut

234   content is removed, the relationship between the mass of the remaining

235   musculoskeletal system and CH_{vol} is more tightly constrained.

236

237   ***Volumetric body mass estimation applied to the dodo***

238   No reliable records of the body mass of dodo exist prior to its extinction in the 17th

239   Century and subsequent mass estimates have varied considerably. Early accounts of

240   the flightless bird suggested an average mass of 50 lb (22 kg) [37], although such

241   accounts "have a tendency towards exaggeration" [10]. More recently a 'slim' dodo

242   (mean 10.2 kg) was proposed on the basis of femoral, tibiotarsal and tarsometatarsal

243   length scaling in modern birds [13]. However hind limb bone length has been shown to

244   correlate poorly with body mass relative to other cross-sectional geometric properties

245   and frequently contains a strong functional signal [38]. Alternatively, a predictive

246   equation based on femoral and tibiotarsal least circumference in ground-dwelling birds

247   has suggested mass estimates between 9.5-12.3 kg [14].

248

249   The application of volumetric mass estimation techniques to the dodo has been rare. A

250   sculpted scale model of a 'slim' dodo based upon mean skeletal measures was created

251   to replicate sketches dating contemporaneously to its survival on Mauritius and resulted

252   in mass estimated of 12.5-16.1 kg [12]. In the same study a 'fat' dodo model based on

253   later 'exaggerated' artworks was predicted to weigh between 21.7-27.8 kg.

254

255   Here we estimate mean eviscerated body masses for articulated composite dodo

256   skeletons of between 8.0-10.8 kg. Without further information regarding the effect of

257   within-subject variability in gizzard, crop or gut content or interspecific scaling of viscera

258   mass, any extrapolation to a live mass should be treated with caution. However, with

259   this caveat in mind, a 33% increase in mass to account for missing organs (as

260   quantified in extant *C. livia*) would take our results to 10.6-14.3 kg. This overlaps with

261   the slim sculpted model based on contemporaneous accounts [12]. Including our 95%

262   confidence intervals takes both the NHM Tring and South Kensington skeletons to a

263   maximum of 18.2 kg and 19.9 kg whole body masses, still considerably below the 22kg

264   suggested historically [37]. In contrast, the 95% confidence intervals of the Edinburgh

265   dodo include 22kg once multiplied by 1.33.

266

267   Unlike all previous volumetric studies, our convex hulling technique does not require a

268   value for body density to be assigned from the literature. Instead we directly derive the

269 relationship between M_b and CH_{vol} in order to avoid uncertainty regarding assigning

270 literature values, which have been shown to differ considerably across avian groups and

271 with various methodologies for estimating body density [17]. However, this does

272 implicitly rely upon the predictive equation being applied to a fossil of an extinct species

273 that is closely related to (and can therefore be assumed to share a similar body density

274 to) the modern dataset from which the predictive equation was derived. In this case of

275 estimating dodo mass based on extant pigeons, we believe this assumption can be

276 upheld. Alternatively, CH_{vol} may be multiplied by a given value of carcass density to give

277 a hard lower limit to body mass (as carcass volume cannot be less than convex hull

278 volume). The sole literature value for intact feathered pigeon density is 648kg/m^3 from

279 Hamershock et al. [39], producing hard lower bounds to estimated body mass 5.8kg,

280 6.3kg, and 7.9kg for the Tring, Kensington and Edinburgh composite skeletons

281 respectively.

282

283 We consider the convex hulling technique to be superior to other sculpting-based

284 volumetric methods (such as manual sculpting with clay [12] or digital sculpting with

285 non-uniform rational B-spline (NURBs) curves [19]) for the purpose of mass estimation

286 as soft tissues and hypothesized respiratory systems need not be reconstructed for

287 fossils of extinct species. When values for centre of mass (COM) and segment inertial

288 properties are required for further biomechanical analyses, NURBs may be required in

289 order to achieve a representative mass distribution across the skeleton. In such

290 situations it is essential that soft tissue reconstructions are based on quantitative

291 comparative dissection data from relevant modern species in order to minimize

292   subjectivity in model creation. However, for the sole purpose of mass estimation,

293   convex hulling should be the preferred technique.

294

295   ***Composite and articulated skeletons***

296   The dodo specimens included in this study are composite skeletons, comprising skeletal

297   material from more than one individual and including sculpted or cast elements.

298   Therefore, our study is limited to estimating the body mass of the hypothetical animal

299   represented by each articulated skeleton, rather than a known individual. Currently

300   there exists only one near-complete dodo skeleton comprising a single individual (the

301   Thirioux dodo), upon which research is currently still continuing [40].

302

303   Whilst the use of composite skeletons should clearly be treated with caution when used

304   in biomechanical analyses, their composite nature does not entirely rule out their use,

305   particularly in the case of mass estimation. A recent large-scale macroevolutionary [41]

306   study of body size in a fossil lineage relied upon mass data derived solely from humeral

307   and femoral circumferences of one individual specimen per species. While this

308   approach is often the only one feasible, given the highly fragmentary nature of the fossil

309   record, taking one individual as being representative of an entire species leaves us

310   vulnerable to the possibility of high levels of intraspecific variation.

311

312   In contrast, a volumetric reconstruction based on a composite skeleton is likely to reflect

313   a species average by virtue of being a combination of several individuals and will be

314   less skewed by isolated robust or gracile elements. If subsequent biomechanical

315 analyses are to be carried out (such as FEA on a particular musculoskeletal unit), then it

316 is important that the body mass entered into the analyses is representative of that

317 specific individual. However, for the case of volumetric body mass estimation alone, a

318 representative species mean can be derived from a composite skeleton.

319

320 Of more concern is the frequency of missing, deformed or reconstructed material within

321 a fossil mount. Known issues with the dodo mounts included in this study include

322 missing ribs (Edinburgh skeleton), missing carpals (NHM South Kensington skeleton),

323 deformation of the fragile pubis (NHM South Kensington skeleton) or the loss of the

324 most of the ischium, pubis and caudal vertebrae (NHM Tring skeleton). For a given

325 object, the extent of the convex hull fitted to that object is dictated solely by its

326 geometric extremes. In many ways this is advantageous for volumetric fossil

327 reconstructions as damage occurring within the bounds of the convex hull does not

328 affect our volume estimate. However when extremities are missing (such as the caudal

329 tip of the pubis), the shape and volume of the convex hull are strongly affected. This is

330 evident in the low percentage trunk volume of the NHM Tring skeleton (Figure 5)

331 compared to those of extant pigeons and other dodos.

332

333 Whilst some evidence of paedomorphosis (retention of juvenile characters as an adult)

334 of pectoral elements and peramorphosis (characters that mature past adulthood) of

335 pelvic elements in the dodo is discernable relative to extant volant pigeons, Figure 5

336 predominantly illustrates the important contribution of trunk volume to total mass

337 estimates. The Edinburgh skeleton has a proportionally more voluminous trunk than that

338   of extant pigeons and other dodo skeletons, and therefore all other skeletal elements

339   contribute proportionally less to total $CH_{vol.}$ The more voluminous trunk relative to other

340   specimens may be attributed to the anterior positioning of the sternum due to

341   constraints associated with the armature supporting the mount. The opposite is true of

342   the NHM Tring skeleton, in which damage to the extremities of the pelvic girdle result in

343   a reduced trunk volume. This highlights the sensitivity of volumetric reconstructions of

344   fossils of extinct species to trunk morphology, and should be a concern when working

345   with both composite and complete fossil specimens.

346 ***Summary***

347 Here we present the first volumetric reconstruction of fossil body mass based entirely on

348 modern whole-animal CT data. The eviscerated body mass of three articulated

349 composite dodo skeletons is estimated to fall between 8.0-10.8 kg. When accounting for

350 missing organ mass, our mean values still fall towards the lower range of previously

351 published mass estimates. As the availability and cost of CT improves, we believe this

352 non-subjective convex hull approach will become increasingly commonplace. Mass

353 estimation of extinct species from fossils relies upon two key components; a reliable

354 calibration equation derived from extant species, and an accurate reconstruction of the

355 extinct individual from its fossil. We discuss the issues surrounding the use of

356 articulated composite skeletons, and highlight the particular importance of trunk

357 morphology to volume reconstructions. We suggest future efforts should focus on

358 quantifying ribcage and sternal geometry in extant groups in order to bracket the

359 possible trunk shape in fossils of extinct species.

360 **Acknowledgements**

361 We thank Zoller+Fröhlich (Z+F) Limited for their continued support, Jennifer Anné and

362 Dr Victoria Egerton (University of Manchester), Martin Baker (University of Liverpool),

363 Malgosia Nowak-Kemp (Oxford Museum of Natural History) and Julian Hume, Judith

364 White and Sandra Chapman (Natural History Museum, London).

References

365   **References**

366   1.   Schmidt-Nielsen K. Scaling: Why is animal size so important? Cambridge:
367   Cambridge University Press; 1984.

368   2.   Turner AH, Pol D, Clarke JA, Erickson GM, Norell MA. A basal dromaeosaurid
369   and size evolution preceding avian flight. Science (80-). 2007;317: 1378–1381.
370   doi:10.1126/science.1144066

371   3.   Boyer AG. Extinction patterns in the avifauna of the Hawaiian islands. Divers
372   Distrib. 2008;14: 509–517. doi:10.1111/j.1472-4642.2007.00459.x

373   4.   Hone DWE, Dyke GJ, Haden M, Benton MJ. Body size evolution in Mesozoic
374   birds. J Evol Biol. 2008;21: 618–624. doi:10.1111/j.1420-9101.2007.01483.x

375   5.   Butler RJ, Goswami A. Body size evolution in Mesozoic birds: Little evidence for
376   Cope's rule. J Evol Biol. 2008;21: 1673–1682. doi:10.1111/j.1420-
377   9101.2008.01594.x

378   6.   Brassey CA, Holdaway RN, Packham AG, Anne J, Manning PL, Sellers WI. More
379   Than One Way of Being a Moa: Differences in Leg Bone Robustness Map
380   Divergent Evolutionary Trajectories in Dinornithidae and Emeidae
381   (Dinornithiformes). PLoS One. 2013;8: e82668.
382   doi:10.1371/journal.pone.0082668

383   7.   Campione NE, Evans DC. A universal scaling relationship between body mass
384   and proximal limb bone dimensions in quadrupedal terrestrial tetrapods. BMC
385   Biol. 2012;10: 60.

386   8.   Field DJ, Lynner C, Brown C, Darroch SAF. Skeletal Correlates for Body Mass
387   Estimation in Modern and Fossil Flying Birds. PLoS One. 2013;8: e82000.
388   doi:10.1371/journal.pone.0082000

389   9.   Cubo J, Arthur W. Patterns of correlated character evolution in flightless birds: a
390   phylogenetic approach. Evol Ecol. 2000;14: 693–702.

391   10.   Hume JP. The history of the Dodo Raphus cucullatus and the penguin of
392   Mauritius. Hist Biol. 2006;18: 65–89.

393   11.   Livezey BC. An ecomorphological review of the dodo (Raphus cucullatus) and
394   solitaire (Pezophaps solitaria), flightless Columbiformes of the Mascarene Islands.
395   J Zool. 1993;230: 247–292.

396   12.   Kitchener AC. The external appearance of the dodo, Raphus cucullatus. Arch Nat
397   Hist. 1993;20: 279–301.

398   13.   Angst D, Buffetaut E, Abourachid A. The end of the fat dodo? A new mass
399   estimate for Raphus cucullatus. Naturwissenschaften. 2011;98: 233–236.

400   14.   Louchart A, Mourer-Chauviré C. The dodo was not so slim : leg dimensions and
401   scaling to body mass. Naturwissenschaften. 2011;98: 357–358.
402   doi:10.1007/s00114-011-0771-6

403   15.   Angst D, Buffetaut E, Abourachid A. In defence of the slim dodo : a reply to
404   Louchart and Mourer-Chauviré. Naturwissenschaften. 2011;98: 359–360.
405   doi:10.1007/s00114-011-0772-5

406   16.   Seebacher F. A new method to calculate allometric length-mass relationships of
407   dinosaurs. J Vertebr Paleontol. 2001;21: 51–60.

408   17.   Hutchinson JR, Ng-Thow-Hing V, Anderson FC. A 3D interactive method for
409   estimating body segmental parameters in animals: Application to the turning and
410   running performance of Tyrannosaurus rex. J Theor Biol. 2007;246: 660–680.

411   18.   Gunga HC, Suthau T, Bellmann A, Stoinski S, Friedrich A, Trippel T, et al. A new
412   body mass estimation of Brachiosaurus brancai Janensch, 1914 mounted and
413   exhibited at the Museum of Natural History (Berlin, Germany). Foss Rec. 2008;11:
414   33–38. doi:10.1002/mmng.200700011

415   19.   Bates KT, Manning PL, Hodgetts D, Sellers WI. Estimating mass properties of
416   dinosaurs using laser imaging and 3D computer modelling. PLoS One. 2009;4:
417   e4532.

418   20.   Allen V, Paxton H, Hutchinson JR. Variation in Center of Mass Estimates for
419   Extant Sauropsids and its Importance for Reconstructing Inertial Properties of
420   Extinct Archosaurs. Anat Rec. 2009;292: 1442–1461.

421   21.   Sellers WI, Hepworth-Bell J, Falkingham PL, Bates KT, Brassey CA, Egerton VM,
422   et al. Minimum convex hull mass estimations of complete mounted skeletons. Biol
423   Lett. 2012;8: 842–845.

424   22.   Brassey CA, Sellers WI. Scaling of convex hull volume to body mass in modern
425   primates, non-primate mammals and birds. PLoS One. 2014;9: e91691.
426   doi:10.1371/journal.pone.0091691

427   23.   Shapiro B, Sibthorpe D, Rambaut A, Austin J, Wragg GM, Bininda-Emonds ORP,
428   et al. Flight of the dodo. Science. 2002;295: 1683.
429   doi:10.1126/science.295.5560.1683

430   24.   CIBC. Seg3D: Volumetric Image Segmentation and Visualization. Scientific
431   Computing and Imaging Institute (SCI). 2014.

432   25.   Barber CB, Dobkin DP, Huhdanpaa HT. The Quickhull algorithm for convex hulls.
433   ACM Trans Math Softw. 1996;22: 469–483.

434   26.   Smith RJ. Use and misuse of the reduced major axis for line-fitting. Am J Phys
435   Anthropol. 2009;140: 476–486.

436   27.   Lavin SR, Karasov WH, Ives AR, Middleton KM, Garland Jr T. Morphometrics of
437   the Avian Small Intestine Compared with That of Nonflying Mammals: A
438   Phylogenetic Approach. Physiol Biochem Zool. 2008;81: 526–550.

439   28.   Johnson KP, de Kort S, Dinwoodey K, Mateman AC, Ten Cate C, Lessells CM, et
440   al. A molecular phylogeny of the dove genera Streptopelia and Columba. Auk.
441   2001;118: 874–887. doi:10.1642/0004-8038(2001)118[0874:AMPOTD]2.0.CO;2

442   29.   Heupink TH, van Grouw H, Lambert DM. The mysterious Spotted Green Pigeon
443   and its relation to the Dodo and its kindred. BMC Evol Biol. 2014;14: 136.
444   doi:10.1186/1471-2148-14-136

445   30.   Falkingham PL. Acquisition of high resolution three-dimensional models using
446   free, open-source, photogrammetric software. Palaeontol Electron. 2012;15: 1T.

447   31.   Mallison H, Wings O. Photogrammetry in Paleontology – A Practical Guide. J
448   Paleontol Tech. 2014;12: 1–31.

449   32.   Wu C. VisualSFM: A visual structure from motion system. [Internet]. 2011.

450   33.   Brassey C, Gardiner J. An advanced shape-fitting algorithm applied to the
451   vertebrate skeleton: improving volumetric mass estimates. R Soc Open Sci.

452   34.   Ibrahim T, Bashrat O. Carcass characteristics of pigeons reared in Bauchi
453   Metropolis, north eastern Nigeria. Anim Prod Res Adv. 2009;5.

454   35.   Omojola AB, Isa MA, Jibir M, S ABTG, Kassim OR, Omotoso AB, et al. Carcass
455   Characteristics and Meat Attributes of Pigeon (Columbia livia) as Influenced by
456   Strain and Sex. J Anim Sci Adv. 2012;2: 475–480.

457   36.   Roth VL. Insular dwarf elephants: a case study in body mass estimation and
458   ecological inferenc. In: Damuth J, MacFadden B, editors. Body size in mammalian
459   paleobiology: Estimates and biological implications. Cambridge: Cambridge
460   University Press; 1990. pp. 151–180.

461   37.   Herbert T. A relation of some yeares' travaile, begunne Anno 1626, into Afrique
462   and the greater Asia, especially the territories of the Persian Monarchie, and
463   some parts of the Oriental Indies and Isles adiacent. London: W Stansby & J
464   Bloome; 1634.

465   38.   Brassey CA, Kitchener AC, Withers PJ, Manning PL, Sellers WI. The Role of
466   Cross-Sectional Geometry, Curvature, and Limb Posture in Maintaining Equal
467   Safety Factors: A Computed Tomography Study. Anat Rec. 2013;296: 395–413.

468   39.   Hamershock DM, Seamans TW, Bernhard GE. Determination of body density for
469   twelve bird species. Flight Dynamics Directorate, Wright Laboratory. Flight
470   Dynamics Directorate, Wright Laboratory; 1993.

471   40.   Randall A, Pepe A, Yamartino K, Kimelblatt A, Claeesens L. How fat was the
472   Dodo? The first mass estimate from digital body reconstruction based on a
473   complete skeleton of Raphus cucullatus. Society of Vertebrate Paleontology
474   Annual Meeting 2014, Berlin Poster Abstract. 2014.

475   41.   Benson RBJ, Campione NE, Carrano MT, Mannion PD, Sullivan C, Upchurch P,
476   et al. Rates of dinosaur body mass evolution indicate 170 million years of
477   sustained ecological innovation on the avian stem lineage. PLoS Biol. 2014;12:
478   e1001853. doi:10.1371/journal.pbio.1001853

479   42.   Rosset A, Spadola L, Ratib O. OsiriX: an open-source software for navigating in
480   multidimensional DICOM images. J Digit Imaging. 2004;17: 205–216.

481   43.   Mascaro J, Litton CM, Hughes RF, Uowolo A, Schnitzer SA. Minimizing Bias in
482   Biomass Allometry : Model Selection and Log-transformation of Data. 2011;43:
483   649–653.

484 Figure 1. Example of the convex hulling process applied to the CT scanned carcass of a
485   Victoria crowned pigeon (*Goura victoria*) from which the skeleton has been
486   segmented. A and C, skeleton in dorsal and lateral view respectively and; B and
487   D, corresponding convex hulls fitted to the functional units of the skeleton. Note
488   convex hulls fitted to the feet in 1D are strongly influenced by the positioning of
489   the toes (see in text for discussion).

490
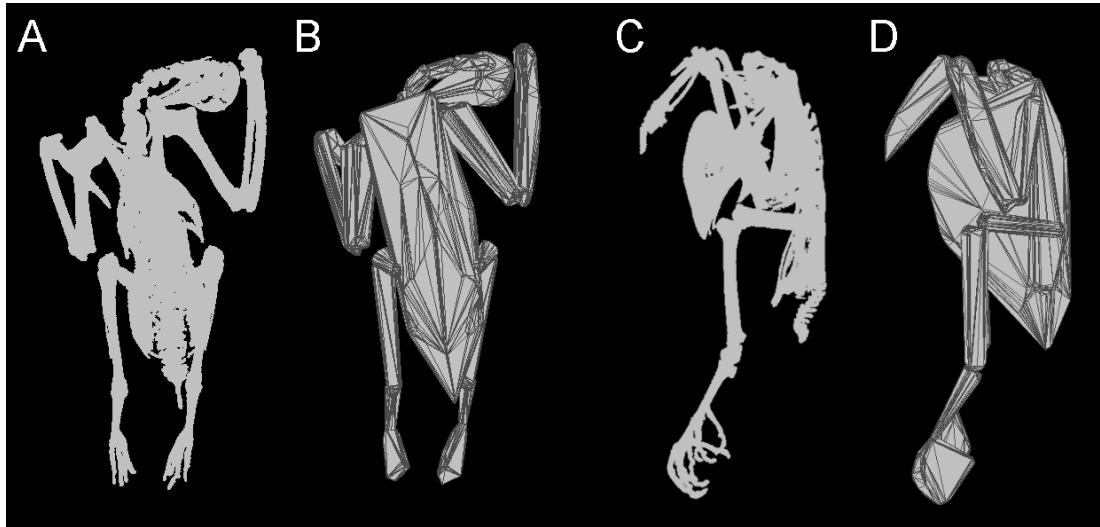
491   Figure 2. OLS regression results. Body mass (g) against convex hull volume (mm^3). For

492   slope equations see Table 2. Filled circles and solid line, eviscerated carcasses;

493   crosses and dashed line, intact carcasses; dot-dash line, combined sample.

494
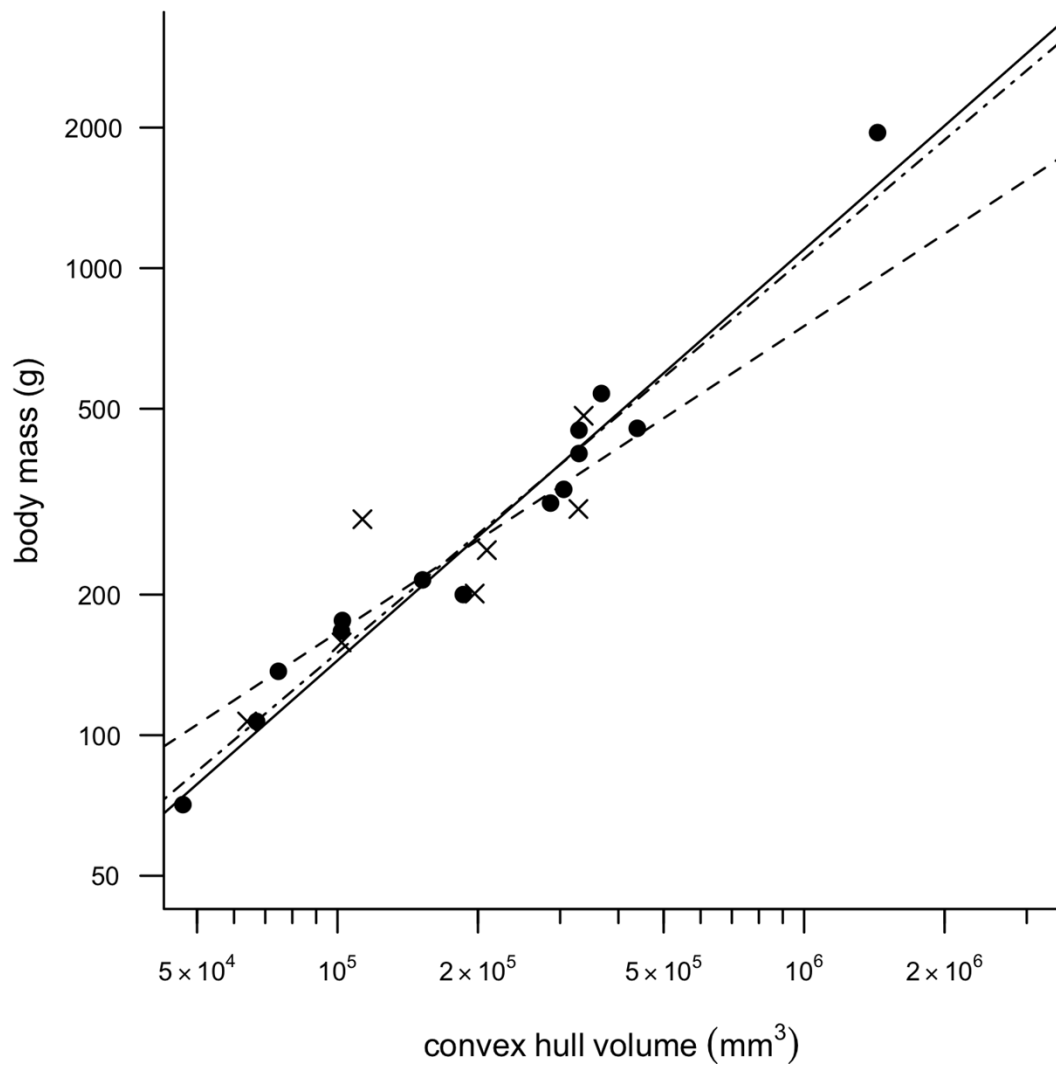
495 Figure 3. A, Photogrammetry model of the Tring dodo skeleton (S/1988.50.1); B,

496 volumetric convex hulls fitted around the skeleton.

497
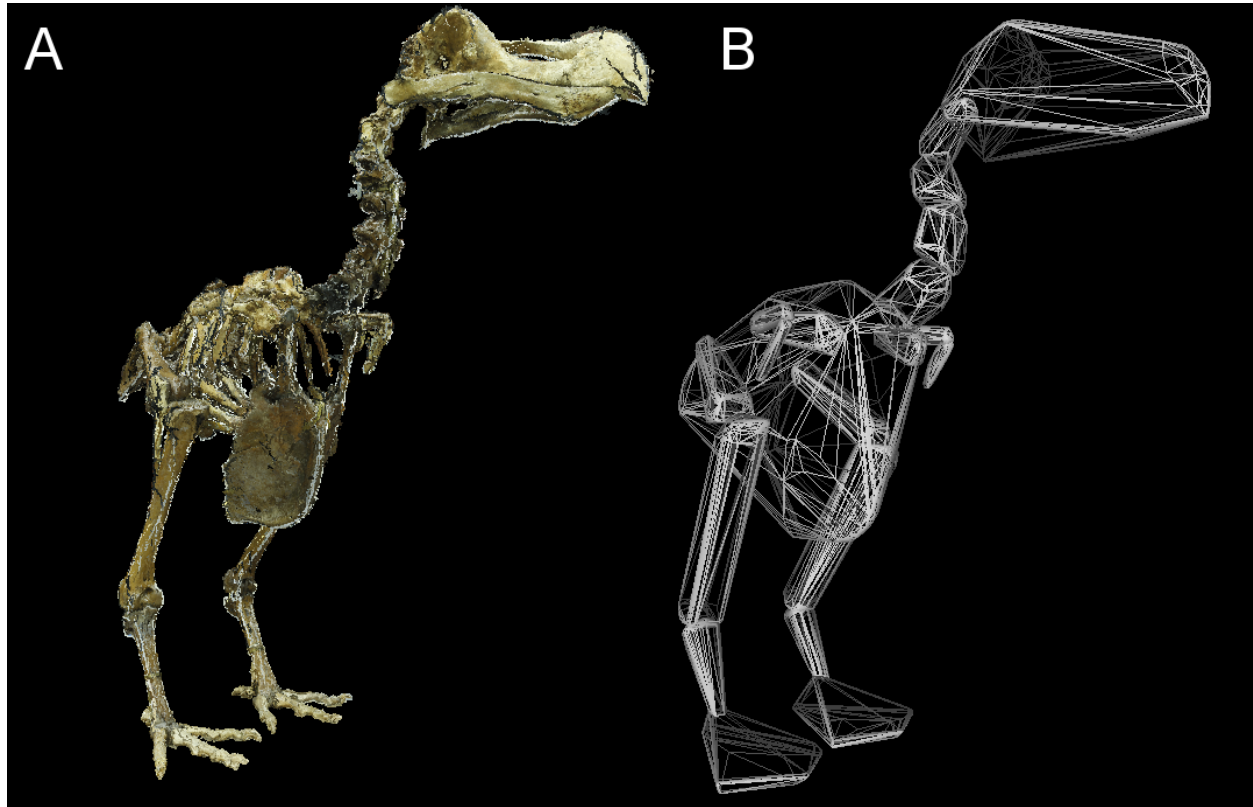
498   Figure 4. The distribution of segment CH_{vol} as a proportion of total CH_{vol} within the

499   convex hulled skeletons of extant pigeons and articulated dodo skeletons. Mean values

500   are illustrated for extant pigeons. Error bars represent 95% confidence intervals of the

501   mean. The underdevelopment of the pectoral girdle (humerus, radius and ulna and

502   carpometacarpals) in dodo relative to extant pigeons is particularly striking.

503
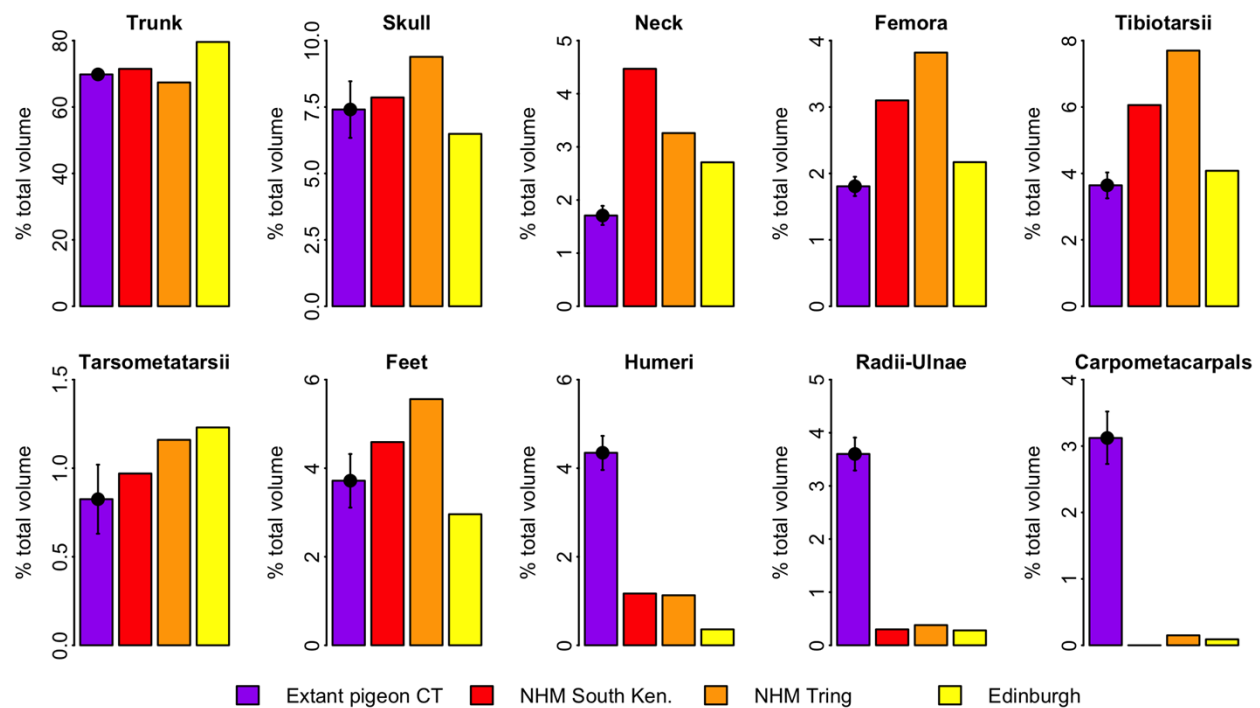
504 Figure 5. Volumetric renderings of a rock dove (*Columba livia, A-B*) and collared dove

505 (*Streptopelia decaocto, C-D)* generated from CT scans. A and C illustrate the outer soft

506 tissue contours of the carcass, while B and D illustrate the position of the gizzard and

507 associated gizzard contents. There is considerable variation in the quantity and size of

508 gizzard stones between intact pigeon specimens within the dataset. Renderings were

509 generated in OsiriX [42]

510

511

Species name	Common name	Body mass (g)	Preparation	CH_{vol} (mm^3)	CH_{vol} – feet (mm^3)
Goura victoria	Victoria crowned pigeon	1951	Eviscerated	1487180	1436777
Streptopelia decaocto*	Collared dove	201	Intact	203875	196791
Columba livia	Rock dove	290	Intact	115945	113074
Columba palumbus*	Wood pigeon	305	Intact	337993	328279
Ducula bicolor	Pied imperial pigeon	450	Eviscerated	337377	329220
Petrophassa rufipennis	Chestnut-quilled rock pigeon	314	Eviscerated	303511	286104
Otidiphaps nobilis	Pheasant pigeon	401	Eviscerated	344368	329238
Nesoenas mayeri	Pink pigeon	200	Eviscerated	197171	185981
Ducula sp.	Imperial pigeon	336	Eviscerated	314985	305344
Caloenas nicobarica	Nicobar pigeon	539	Eviscerated	383736	367753
Phaps chalcoptera	Common bronze-winged pigeon	249	Intact	213953	208942
Ducula aenea	Green imperial pigeon	483	Intact	348268	336968
Columba guinea	Speckled pigeon	158	Intact	105156	102041
Zenaida graysoni	Socorro dove	176	Eviscerated	105776	102441

Gallicolumba sp.	Bleeding heart dove	215	Eviscerated	163764	152136
Phapitreron leucotis	White-eared brown dove	107	Eviscerated	69424	67088
Ptilinopus sp.	Fruit dove	71	Eviscerated	47816	46635
Ptilinopus superbus	Superb fruit dove	137	Eviscerated	77882	74691
Treron vernans	Pink-necked green pigeon	167	Eviscerated	104991	101984
Ocyphaps lophotes	Crested pigeon	107	Intact	67451	64011

512   Table 1. Specimen list of modern pigeons sourced from National Museums Scotland, Edinburgh. CH_{vol}, minimum convex

513   hull volume of the skeleton; CH_{vol} – feet, minimum convex hull volume minus the volume of the feet. * indicates specimens

514   were sourced from the University of Manchester. All other specimens were loaned from National Museums Scotland,

515   Edinburgh.

516

517

518

Model	a	a ($\pm$95%)	b	b ($\pm$95%)	r^2	p	MSE	AIC_{OLS}	AIC_{PGLS}
Eviscerated	-2.31	-2.90 - -1.72	0.89	0.78-1.00	0.97	<0.001	0.0049	-28.42	-24.66

- minus feet	-2.31	-2.87 - -1.74	0.90	0.79-1.00	0.97	<0.001	0.0046	-29.38	-25.35
Intact	-1.08	-3.69 - -1.53	0.66	0.16-1.16	0.70	0.019	0.0163	-5.29	-9.76
- minus feet	-1.06	-3.62 - -1.50	0.66	0.17-1.15	0.70	0.018	0.0161	-5.41	-10.03
Combined	-2.08	-2.75 - -1.42	0.85	0.72-0.98	0.92	<0.001	0.0086	-34.42	-30.12
- minus feet	-2.08	-2.73 - -1.42	0.85	0.73-0.98	0.92	<0.001	0.0084	-34.94	-30.46

519 Table 2. Ordinary least squares regressions of $\log_{10}$ body mass (g) against $\log_{10}$ convex hull volume (CH_{vol}, mm^3). ±95%,

520 95% confidence intervals of the intercept and slope; MSE, mean square error of the regression; AIC, Akaike Information

521 Criterion calculated for Ordinary Least Squares (OLS) and Phylogenetically Generalised Least Squares (PGLS).

522

523

524

Model	Accession number	CH_{vol} (mm^3)	CH_{vol} – feet (mm^3)	Eviscerated M_b (g) *	95% PI (g)
NHM Tring dodo	S/1988.50.1	8942820	8445134	7980	4653- 13685
NHM Kensington dodo	NHM A.9040	9730367	9283795	8687	5027-15011

Edinburgh dodo	NMS.Z.1993.13	12147000	11787000	10760	6106-18961

525 Table 3. M_b estimated using 'eviscerated' equation minus feet (Table 2) and applying correction factor $e(MSE/2)$ to

526 account for back-transformation of a log-linear model into a power function [43], where MSE is the mean square error

527 reported in Table 2. 95%PI, 95% prediction intervals.

528

529

530

531

532